MJSAT

Malaysian Journal of Science and Advanced Technology

journal homepage: https://mjsat.com.my/

Antibacterial and Cytotoxicity Study of Nanoporous Hydroxyapatite Doped with Euphorbia tirucalli L. Extract

Mangalagowri Sangar¹, Nur Farahiyah Mohammad¹, Nashrul Fazli Mohd Nasir¹, Khairul Farihan Kasim³, Siti Shuhadah Md Saleh³, and Farah Diana Mohd Daud⁵

- ¹ Faculty of Electronic Engineering & Technology, Universiti Malaysia Perlis, Pauh Putra, 02600 Arau, Perlis, Malaysia.
- ² Medical Device and Life Science Cluster, Sport Engineering Research Centre (SERC), Universiti Malaysia Perlis, Pauh Putra, 02600 Arau, Perlis, Malaysia.
- ³ Faculty of Chemical Engineering & Technology, Universiti Malaysia Perlis, Jejawi 2, 02600 Arau, Perlis, Malaysia.
- ⁴ Biomedical and Nanotechnology Research Group, Centre of Excellence Geopolymer and Green Technology (CEGeoTech), Universiti Malaysia Perlis, Jejawi, 02600 Arau, Perlis, Malaysia.
- ⁵ Manufacturing and Materials Engineering Department, Kuliyyah Engineering, International Islamic University Malaysia (IIUM), Jalan Gombak, 53100 Kuala Lumpur, Malaysia.

KEYWORDS

Euphorbia tirucalli Hydroxyapatite (HA) Antibacterial properties Bioactive compounds Bone tissue engineering

ARTICLE HISTORY

Received 11 August 2025 Received in revised form 2 October 2025 Accepted 20 October 2025 Available online 3 November 2025

ABSTRACT

This study investigates the characterization, and biomedical potential of Euphorbia tirucalli L. (E.tirucalli L.) extract, focusing on its bioactive compounds, antibacterial properties, and incorporation into hydroxyapatite (HA) for biomedical applications. High-Performance Liquid Chromatography (HPLC) analysis confirmed gallic acid as the predominant phenolic compound in the extract (557.9 ± 8.3 mg/g). Antibacterial testing revealed that DHA 25% exhibited the highest inhibition zones against Staphylococcus aureus (S. aureus) (7.07 ± 0.41) cm²) and Escherichia coli (E. coli) (3.14 \pm 0.51 cm²), indicating enhanced antibacterial activity at higher doping concentrations. Cytotoxicity assays demonstrated that DHA 25% promoted cell proliferation (120.0 \pm 5.3% on day 7), confirming its biocompatibility for bone tissue engineering. X-ray diffraction (XRD) revealed that E.tirucalli L. doping affected HA crystallinity, potentially improving bioresorption and osteoconductivity. Fourier-Transform Infrared Spectroscopy (FTIR) confirmed the successful incorporation of E.tirucalli L. into HA, while Scanning Electron Microscopy (FESEM) showed increased agglomeration and reduced porosity at higher doping concentrations. The integration of E. tirucalli L. extract into HA introduces natural bioactive compounds, such as gallic acid, that enhance antibacterial, antioxidant, and biocompatible properties beyond conventional inorganic doping approaches. In conclusion, E. tirucalli L.-doped hydroxyapatite demonstrates great potential for applications in bone regeneration and implant technology due to its enhanced antibacterial and biocompatible properties, with the possibility of future exploration for controlled drug release applications.

© 2025 The Authors. Published by Penteract Technology.

This is an open access article under the CC BY-NC 4.0 license (https://creativecommons.org/licenses/by-nc/4.0/).

1. Introduction

Bioceramics have emerged as vital materials in the biomedical field, particularly for applications in bone and dental implants due to their inherent biocompatibility and functionality. Among them, hydroxyapatite (HA), a naturally occurring calcium phosphate mineral with the chemical formula Ca₁₀(PO₄)₆(OH)₂, stands out for its close resemblance to the

mineral component of bone. Owing to its biocompatibility, bioactivity, and non-toxicity, HA has been widely utilized in bone tissue engineering and regenerative medicine [1]. Its ability to support bone regeneration stems from its osteoconductive, osteointegrative, and osteoinductive properties, which are crucial for promoting bone repair [2]. As a result, HA is extensively used in bone substitute applications, including implant coatings and bone defect fillers [3].

E-mail address: Nur Farahiyah Mohammad < farahiyah@unimap.edu.my >. https://doi.org/10.56532/mjsat.v5i4.588

 $2785\text{-}8901/\ \text{\ensuremath{\mathbb{C}}}\ 2025$ The Authors. Published by Penteract Technology.

^{*}Corresponding author:

Despite its advantages, pure HA exhibits limitations, including poor mechanical strength, limited resorption, inadequate antibacterial properties, and suboptimal drugloading efficiency. To overcome these drawbacks, researchers have investigated doping HA with various agents, particularly metal ions such as Ag⁺, Cu²⁺, Zn²⁺, Ti⁴⁺, Mg²⁺, Fe^{2+/3+}, Sr²⁺, and Ce^{3+/4+}, to enhance its antibacterial and mechanical performance [4]. While metal doping can improve HA properties, it may also alter its structural and chemical characteristics, such as crystallinity, morphology, and biocompatibility, which necessitates detailed characterization.

In response to concerns over metal-induced cytotoxicity and antibiotic resistance, plant-based doping agents have gained interest. *E.tirucalli* L., commonly known as the pencil plant, is rich in polyphenols with well-documented antibacterial, antioxidant, anti-inflammatory, and anticancer properties [5]. Polyphenolic compounds like gallic acid, ellagic acid, and quercetin are known to disrupt bacterial cell membranes and inhibit bacterial enzymes, making them promising candidates for improving HA's antibacterial performance. Notably, polyphenols from *E. tirucalli* L. have shown efficacy against common pathogens such as Staphylococcus aureus and Escherichia coli, which are often responsible for implant-related infections [6]. These infections are increasingly difficult to treat due to the rise of antibiotic-resistant strains, which pose a serious threat to implant success.

E.tirucalli L. was chosen for this study due to its wellbroad-spectrum antibacterial documented properties, particularly its effective inhibition of clinically relevant pathogens such as Staphylococcus aureus and Escherichia coli, which are common causes of bone implant-associated infections [7]. The plant's bioactive components, including flavonoids, tannins, and phenolic compounds like gallic acid, contribute to its antibacterial efficacy by disrupting microbial membranes, inactivating adhesion factors, and interfering with microbial enzymes [8]. Compared to other bioactive plants, E. tirucalli's distinct combination of potent antimicrobial activity, high content of therapeutic phytochemicals, and historical medicinal use as a natural antimicrobial agent provide a strong rationale for its specific selection as a doping agent in hydroxyapatite, aiming to develop multifunctional biomaterials that combine infection control with bone regenerative properties[5]. This specificity in antibacterial effectiveness and rich bioactive profile distinguishes E. tirucalli L. as an ideal candidate over other plant extracts with known bioactivity.

Several studies have highlighted the antimicrobial, antioxidant, and anticancer activities of Euphorbia tirucalli, primarily based on in vitro assays [5],[39]. However, these findings are largely preliminary, with notable variability in results due to differences in extraction methods and solvent systems, which impact phytochemical yields and limit comparability. Unlike other medicinal plants such as Camellia sinensis (green tea), Curcuma longa (curcumin), and Azadirachta indica (neem), which have been widely studied and successfully applied in hydroxyapatite (HA) modification for biomedical applications [44],[45] research on incorporating E. tirucalli into biomaterials remains scarce. This gap underscores both the novelty and necessity of the current work, which critically extends beyond existing phytochemical studies to evaluate the feasibility and efficacy of E. tirucalli extract as a natural bioactive dopant in a bone-regenerative HA system. By doing so, the study aims to harness E. tirucalli's welldocumented antimicrobial potential in a clinically relevant bone biomaterial context.

The novelty of this study lies in the successful incorporation of Euphorbia tirucalli L. extract, rich in bioactive phenolic compounds such as gallic acid, into hydroxyapatite (HA) to create a multifunctional biomaterial with enhanced antibacterial, biocompatible, and structural properties. Unlike conventional doping methods that primarily use metal ions, this work introduces a natural, plant-based doping agent that not only modulates HA crystallinity and porosity for improved bioresorption and osteoconductivity but also imparts significant antibacterial activity against key pathogens and promotes cell proliferation. This bioactive plant extract doping advances HA biomaterials by enhancing biological performance and may offer potential for future drug delivery applications, representing a novel approach in bone tissue engineering and implant technologies that integrates natural therapeutic agents with inorganic matrices for superior regenerative outcomes. Although previous studies have demonstrated the antibacterial and antioxidant activity of E. tirucalli L., limited research has explored its incorporation into HA, particularly using Soxhlet extraction, which may yield higher concentrations of active compounds [7]. Therefore, the objectives of this study are to: (i) extract, identify, and quantify polyphenolic compounds from E. tirucalli L. using Soxhlet extraction, (ii) incorporate the plant extract into HA to develop a novel doped biomaterial, (iii) characterize the structural, morphological, and chemical changes induced by the doping process, and (iv) evaluate the antibacterial and biocompatibility performance of the extractdoped HA for potential bone implant applications.

2. METHODOLOGY

2.1 Sample preparation

Aerial parts of *Euphorbia tirucalli* L. were cleaned, dried at $50\,^{\circ}\text{C}$ for 72 hours, powdered, and stored at $-21\,^{\circ}\text{C}$. Soxhlet extraction (9 g, 200 mL ethanol, 90 °C, 20 cycles) was performed. The extract was concentrated, dried, and partitioned with hexane and DCM. Fractions were evaporated and stored at $-21\,^{\circ}\text{C}$.

2.2 Identification and Quantification of Phenolic Compounds Using HPLC

Phenolic compounds in the extracts were identified and quantified using High-Performance Liquid Chromatography (HPLC), following a modified method from [5]. The HPLC column was maintained at 35 °C, and detection was performed at 253 nm. A 40 μL sample was injected with a 1.0 mL/min flow rate. The mobile phase consisted of acetonitrile (A) and aqueous acetic acid (B) with gradient elution: 80:20 A:B (5 min), 50:50 (7 min), and 28:72 (20 min). Standards used included gallic acid, quercetin, and ferulic acid. Retention times and spectra were compared to known standards. Calibration curves and peak purity ensured accurate quantification using HPLC software.

2.3 Synthesis and Preparation of HA Doped with E. tirucalli L. Extract

Nanoporous hydroxyapatite (HA) was synthesized via wet chemical precipitation. Calcium nitrate tetrahydrate (9.45 g) and P123 (3 g) were dissolved in distilled water to create porosity. Diammonium hydrogen phosphate (3.17 g) was added

dropwise, with pH maintained at 11 using 1 M NaOH. The mixture was aged, centrifuged, washed, dried, ground, and calcined at 550 °C. For doping, 3 g HA was mixed with 10 mL of 5 mg/mL (5%), 15mg/mL (15%) and 25 mg/mL (25%) of *E. tirucalli* extract, shaken for 24 h, filtered, vacuum-dried, and ground. Pellets (10 mm diameter, 2 mm thick) were formed using 0.3 g of doped HA pressed at 175 MPa for 6 cycles for antibacterial testing. The doping concentrations of 5%, 15%, and 25% *Euphorbia tirucalli* extract in hydroxyapatite were selected based on a combination of factors rather than arbitrary choice. These concentrations reflect a balance between maximizing bioactive phytochemical incorporation for antibacterial and regenerative benefits while avoiding excessive doping that could compromise material stability or biocompatibility.

2.4 X-Ray Diffraction (XRD) Spectrometry

X-ray Diffraction (XRD) analysis was performed using a Bruker AXS D8 diffractometer to examine the crystallographic structure and phase composition of synthesized samples. Approximately 1 gram of powdered material was analyzed over a Bragg angle range of 10° to 90° using CuK α radiation (λ = 0.15406 nm). Phase composition, crystallinity, and crystallite size was determined using X'pert Highscore Plus software. Crystallinity (Xc) was calculated from the intensity of the (300) reflection peak, and crystallite size (Xs) was determined using Scherrer's equation [8].

2.5 Fourier Transform Infrared (FTIR) Spectroscopy

The identification and verification of functional groups present in HA powders were carried out using FTIR analysis. The FTIR measurements were performed with a Perkin Elmer Spectrum 65 model, covering a *frequency* range from 400 cm⁻¹ to 4000 cm⁻¹.

2.6 N₂ Adsorption-Desorption Isotherms and BJH Pore Size Distribution

Surface area and porosity of hydroxyapatite (HA) and *E. tirucalli*-doped HA (DHA) were evaluated using BET nitrogen adsorption-desorption analysis with a Micromeritics ASAP 2020 analyzer. Samples were degassed at 150 °C for 12 hours to eliminate moisture *and* gases. Nitrogen adsorption was performed at 77 K using 0.1–0.2 g of each sample, with isotherms recorded over a relative pressure range of 0.05–0.99. BET surface area was calculated from the linear region (P/P₀ = 0.05–0.30), while BJH analysis on the desorption branch provided pore size distribution and total pore volume. Results highlighted how *E. tirucalli* doping alters HA's surface and pore characteristics.

2.7 Morphological Analysis using Field Emission Scanning Electron Microscope (FESEM)

Field emission scanning electron microscopy (FESEM) (Carl Zeiss, Germany) was employed to analyze the morphology and particle size. A drop of both doped and pure hydroxyapatite powder was placed on a gold grid and examined under the microscope at a voltage of 15 kV, with magnifications ranging from 1,000x to 150,000x, to capture detailed electron images of the particles.

2.8 Agar Well Diffusion Method

The agar disc diffusion method was used to test the antibacterial activity of HA pellets against bacteria. Inoculum was mixed with nutrient agar (NA) at a temperature below 37°C to avoid killing the bacteria. The mixture was poured into a petri

dish, and HA pellets was immersed in the agar before it solidifies. After labeling and closing the dish, it was incubated at 37°C for 24 hours. The bacteria growth was observed and recorded after incubation [9].

2.9 Proliferation and Cytotoxicity Test

The proliferation and cytotoxicity of scaffolds were evaluated using the MTT assay through a direct contact method on B2B human airway epithelial cells, selected for preliminary cytocompatibility screening. Cells were seeded at a density of 500 cells per well onto sterilized scaffolds weighing 0.04–0.05 which were pre-soaked in Alpha-DMEM media supplemented with 10% fetal bovine serum, penicillin, and streptomycin. The assay was performed in triplicate (n=3) with appropriate negative controls (cells cultured without scaffolds) and positive controls (cells exposed to known cytotoxic agents). Optical density readings were taken at 570 nm on days 1, 3, 5, and 7, with results statistically analyzed using one-way ANOVA and significance set at p < 0.05. While the B2B cell line is not typically bone-specific but the available cell line in laboratory behave similarly in basic cytotoxicity or proliferation assays. This approach offers a robust assessment of scaffold biocompatibility and proliferation potential.

3. RESULTS AND DISCUSSION

3.1 High Performance Liquid Chromatography

The HPLC analysis of *Euphorbia tirucalli* extracts, subjected to different solvents—dichloromethane, hexane, and aqueous ethanol—revealed distinct variations in phytochemical content. This approach is crucial for determining the most effective solvent for extracting antioxidants from the plant material [5].

Table 1. Quantified levels of four key polyphenols: ellagic acid, gallic acid, quercetin, and ferulic acid.

Solvent Standard	Dichloromethane (mg/g)	Hexane (mg/g)	Aqueous ethanol (mg/g)
Ellagic acid	$15.7\pm0.5^{\rm a}$	34.9 ± 1.2^{b}	$305.3 \pm 5.6^{\circ}$
Gallic acid	$0.0\pm0.0^{\mathrm{a}}$	$40.8\pm1.8^{\rm b}$	$557.9 \pm 8.3^{\circ}$
Quercetin	$0.0\pm0.0^{\mathrm{a}}$	$5.5\pm0.3^{\rm b}$	$156.7 \pm 4.2^{\circ}$
Ferulic acid	$8.5 \pm 0.4^{\mathrm{a}}$	$9.5\pm0.7^{\rm a}$	61.4 ± 2.1^{b}

* Values are shown as mean and standard deviation, Different letters (a, b,c) mean significant differences (p < 0.05).

Ellagic acid, a polyphenol with four hydroxyl groups and two lactone rings, is recognized for its robust antioxidant activity through free radical scavenging and enzyme activation. It offers anti-inflammatory, anticancer, and antibacterial effects [12]. Its concentration was lowest in dichloromethane (15.7 mg/g), higher in hexane (34.9 mg/g), and significantly higher in aqueous ethanol (305.3 mg/g). Ethanol's intermediate polarity enables better solubility and penetration into plant matrices, making it the most efficient solvent [13].

Gallic acid, known for its strong radical scavenging due to its three adjacent hydroxyl groups, exhibits notable antibacterial and anticancer properties and may protect against cardiovascular and neurodegenerative diseases [14]. It was not detectable in the dichloromethane extract, while hexane and

ethanol extracts yielded 40.8 mg/g and 557.9 mg/g, respectively, further confirming ethanol's superior efficiency [13].

Quercetin, a flavonoid with multiple hydroxyl groups and a conjugated ring system, offers antioxidant effects by scavenging reactive oxygen and nitrogen species, metal chelation, and hydrogen donation [15]. Quercetin was absent in dichloromethane, detected at 5.5 mg/g in hexane, and peaked at 156.7 mg/g in ethanol, again confirming ethanol's suitability for polar phytochemicals.

Ferulic acid, with a methoxy group and conjugated double bond, neutralizes free radicals and inhibits lipid peroxidation. Its antioxidant and anti-inflammatory properties are linked to disease prevention, including neurodegenerative disorders and cancer [16]. It was found in all extracts—8.5 mg/g (dichloromethane), 9.5 mg/g (hexane), and 61.4 mg/g (ethanol) showing consistent improvement with ethanol [5]. In conclusion, ethanol was the most effective solvent in extracting polyphenols from *E. tirucalli*, particularly gallic acid and quercetin. These findings align with previous studies supporting ethanol's efficiency in extracting antioxidant compounds from plant matrices [13],[14],[15].

3.2 X-Ray Diffraction (XRD) Spectrometry

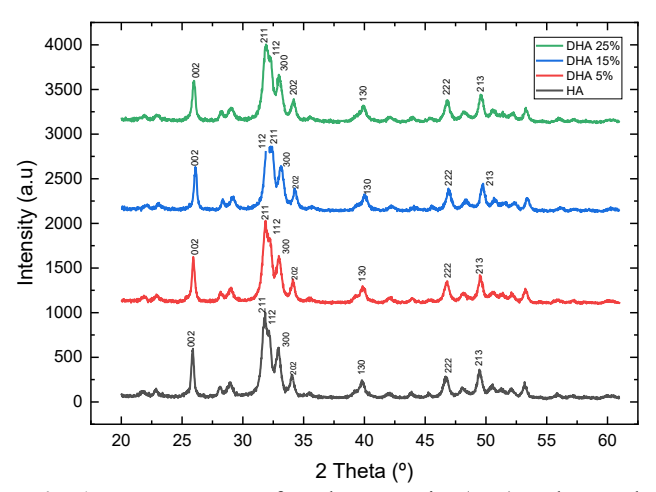


Fig. 1. XRD patterns of Hydroxyapatite (HA) and Doped Hydroxyapatite (DHA)

X-ray diffraction (XRD) analysis confirmed that hydroxyapatite (HA) and *E. tirucalli*-doped HA (DHA) retained key HA peaks in agreement with PDF 01-074-0565, notably at $2\theta = 25.90^{\circ}$ (002), 31.80° (211), 32.20° (112), 32.90° (300), and 34.10° (202), among others. Pure HA showed the highest crystallinity at 42%, while DHA 5%, 15%, and 25% exhibited 37%, 28%, and 25%, respectively. The reduction in peak sharpness and intensity with increasing extract concentration suggests structural disruption of HA crystals. These changes may enhance bioactivity and resorption but reduce mechanical strength [17],[18]. [19].

3.3 Fourier Transform Infrared (FTIR) Spectroscopy

FTIR spectroscopy was utilized to characterize the functional groups present in pure hydroxyapatite (HA), *Euphorbia tirucalli* extract (EXT), and doped hydroxyapatite (DHA) with 5%, 15%, and 25% extract concentrations. The resulting spectra (Figure 3.1) confirm the successful incorporation of the extract into the HA matrix.

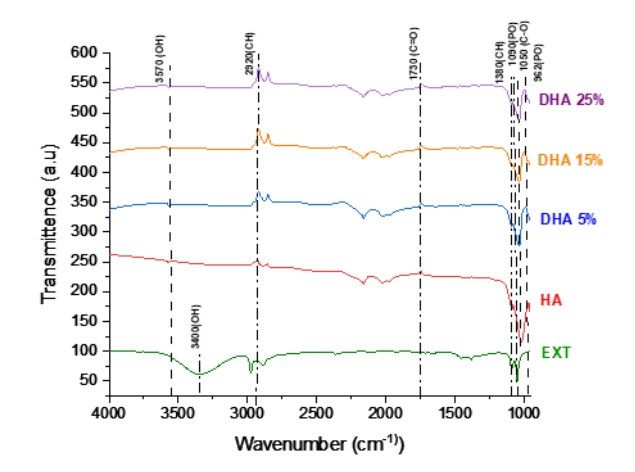


Fig. 2. FTIR spectrum of hydroxyapatite (HA) doped with Euphorbia tirucalli extract

Fourier Transform Infrared (FTIR) spectroscopy confirmed the successful incorporation of E. tirucalli extract into the hydroxyapatite (HA) matrix. The DHA spectra showed a combination of peaks from both HA and the extract. Retention of characteristic phosphate (PO₄³⁻) and hydroxyl (OH⁻) peaks at ~1090, 1040, 962, 600, 570, 3570, and 630 cm⁻¹ indicates preservation of HA's structure despite extract doping [20],[21]. The extract contributed additional peaks: O-H stretching $(\sim 3400 \text{ cm}^{-1})$, C-H stretching $(\sim 2920 \text{ cm}^{-1})$, C=O $(\sim 1730 \text{ cm}^{-1})$ cm⁻¹), C=C (~1630 cm⁻¹), C-H bending (~1380 cm⁻¹), and C-O stretching (~1050 cm⁻¹), indicating the presence of hydroxyl, aliphatic chains, esters, aromatics, and [22],[23],[24]. As extract concentration increased, the O-H and C=O peak intensities also increased, confirming effective doping. Slight reductions in P-O peak intensities suggest molecular interactions but not structural degradation. A unique peak at 1380 cm⁻¹ in DHA 15% supports optimal doping [25]. These findings confirm that E. tirucalli extract was successfully incorporated without compromising the HA structure, creating a biofunctional composite with enhanced potential for biomedical use [26].

3.4 N₂ Adsorption-Desorption Isotherms and BJH Pore Size Distribution

The Barrett-Joyner-Halenda (BJH) pore size distribution analysis provides insights into the pore structure of hydroxyapatite (HA) and *Euphorbia tirucalli*-doped HA (DHA) at 5%, 15%, and 25% concentrations. The graph shown in Figure 3.3 plotting differential pore volume against pore diameter reveals the effect of doping on the porosity of the material.

Pore size distribution is a critical parameter in bone tissue engineering, as it influences cell attachment, nutrient diffusion, and tissue integration [27]. For all samples, including pure HA and DHA variants, the most prominent peak lies within the 40–50 nm range, indicating a dominant mesoporous structure. According to IUPAC classification (1985), pores are classified as micropores (<2 nm), mesopores (2–50 nm), and macropores (>50 nm). Mesopores are particularly beneficial for bone regeneration as they support vascularization and bone ingrowth [17].

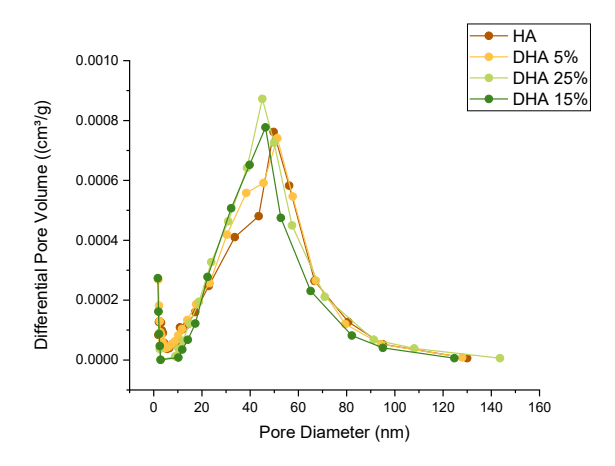


Fig. 3. BJH pore size distribution of Hydroxyapatite (HA) and Doped Hydroxyapatite (DHA)

Table 2. BET Analysis for Hydroxyapatite (HA) and *Euphorbia tirucalli* Doped Hydroxyapatite (DHA)

Sample	Surface	ВЈН	ВЈН	Pore
	area	Adsorption	Desorption	volume
	(m^2g^{-1})	average	pore width	(cm3/g)
		pore width	(nm)	
		(nm)		
	25 (2((21.550	21 155	0.20004
Pure	35.6266	31.550	31.155	0.29994
HA				
DHA	35.7340	36.002	30.810	0.29275
5%				
DHA	28.1795	43.474	39.780	0.29994
15%				
DHA	25.5867	41.413	35.870	0.25748
25%				

BET and BJH analyses demonstrated that doping hydroxyapatite (HA) with Euphorbia tirucalli extract significantly affects its surface area and pore characteristics. Pure HA exhibited a surface area of 35.6266 m²/g and a pore volume of 0.29994 cm³/g. Doping with 5% and 15% extract led to slight changes in surface area but noticeable increases in pore width. DHA 25% displayed reduced surface area (25.5867 m²/g) but greater BJH pore width, suggesting enhanced mesoporosity due to pore fusion or expansion. Notably, DHA 25% exhibited a slightly more prominent peak, indicating increased mesopore formation which may enhance cell adhesion and proliferation [28]. The decreasing surface area combined with increasing pore size upon higher doping of hydroxyapatite (HA) with Euphorbia tirucalli extract can be explained by structural changes induced during doping. As the plant extract is incorporated, its bioactive compounds may cause fusion or expansion of smaller pores into larger mesopores, leading to pore coalescence [28]. This structural rearrangement reduces the overall specific surface area because fewer total pores exist but with larger dimensions. The larger pores create more spacious channels for nutrient flow and cell migration, which benefit bone tissue regeneration, despite the surface area decline [29]. Additionally, the presence of organic extract molecules can partially block or fill finer pores, contributing to surface area reduction but enhancing mesoporosity, thus improving cell adhesion and proliferation sites in a size range more physiologically relevant for tissue ingrowth. This trade-off between surface area and pore size optimizes the scaffold architecture for bone regeneration applications. All samples showed Type IV isotherms with H1 hysteresis loops [29], confirming the presence of mesoporous structures suitable for capillary condensation. Such porosity facilitates nutrient diffusion, vascularization, and cell migration, making DHA favorable for bone regeneration [30],[31],[32].

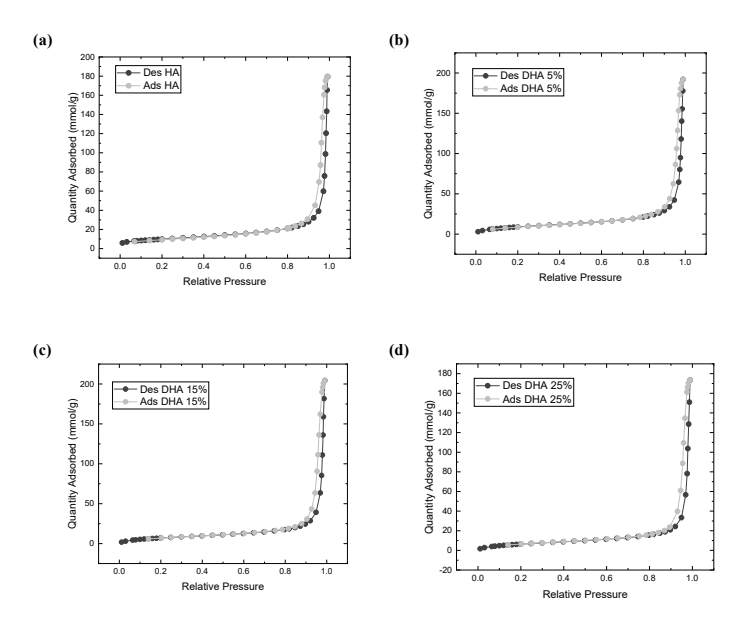


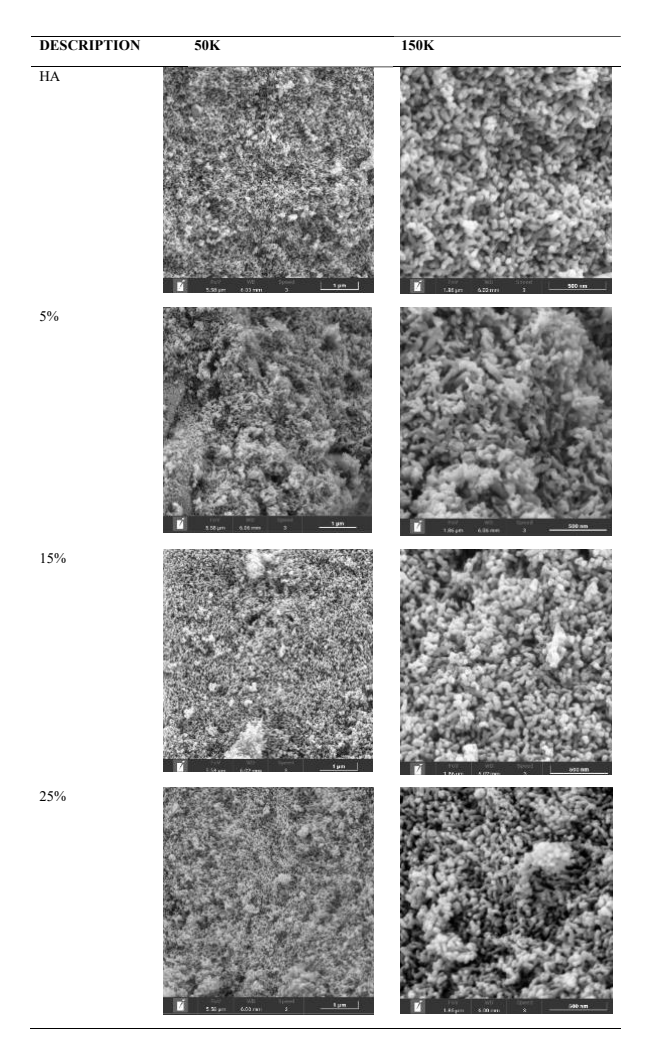
Fig. 4. Adsorption-desorption isotherms of (a) HA, (b) DHA 5%, (c) DHA 15%, and (d) DHA 25%

3.5 Field Emission Scanning Electron Microscopy (FESEM)

Field Emission Scanning Electron Microscopy (FESEM) was employed at magnifications of 50K and 150K to evaluate the morphological characteristics of pure hydroxyapatite (HA) and HA doped with *E.tirucalli L.* extract at 5%, 15%, and 25% concentrations. The analysis focused on particle size, shape, distribution, aggregation, and porosity critical factors influencing the material's suitability for biomedical applications.

FESEM images in Table 3 revealed notable morphological differences between pure and doped hydroxyapatite (HA) samples. Pure HA displayed irregular, interconnected particles and rod-like structures with high porosity at 50K and 150K magnifications, respectively, aligning with findings by [33], [[34]. Upon doping with 5% E.tirucalli extract, particles showed denser packing and aggregation, likely due to enhanced interactions [35].

Table 3. Field Emission Scanning Electron Microscopy (FESEM) Images of HA and Doped Samples at Different Magnifications (50K and 150K)



The 15% doped sample exhibited smaller, more uniform particles and significantly reduced porosity, indicating compactness. The most pronounced changes occurred at 25% doping, where particles appeared fused and boundaries indistinct, suggesting advanced coalescence and densification. These structural shifts reduce porosity and increase agglomeration. Such morphology especially rod-like particles with reduced porosity enhances osteoconductivity and mechanical properties, as supported by [30]. In a biomedical context, changes observed in characterization techniques such as X-ray diffraction (XRD), Fourier-transform infrared spectroscopy (FTIR), and Brunauer-Emmett-Teller (BET) analyses offer critical insights into the performance of biomaterials. For instance, alterations in HA crystallinity detected by XRD can influence its bioresorption rate; decreased crystallinity often leads to higher solubility and faster degradation, which can enhance bone remodeling and integration by allowing the scaffold to be gradually replaced by new bone tissue. FTIR spectra revealing shifts or intensities in phosphate, hydroxyl, and carbonate groups help confirm chemical composition and functional group incorporation, which affect bioactivity, cell adhesion, and mineralization processes crucial for bone regeneration. Additionally, BET

surface area and porosity measurements inform on the scaffold's microstructure; higher surface area and suitable pore size distribution improve protein adsorption, nutrient diffusion, and vascularization, promoting osteoconductivity and tissue ingrowth. Together, these characterization outcomes are essential to understand how structural and chemical modifications translate to improved biological performance and successful implant integration [34]. Overall, increasing extract concentration altered particle interaction, promoting denser packing. As shown in Table 3.11, 15% and 25% DHA samples exhibit promising mesoporosity for bone tissue applications.

3.6 Antibacterial Properties of Doped HA

The antibacterial activity of *E.tirucalli* L. extract-doped hydroxyapatite (HA) was evaluated using the well-diffusion method against *Escherichia coli* (*E. coli*) and *Staphylococcus aureus* (*S. aureus*). Three concentrations of *E.tirucalli* L. extract (5%, 15%, and 25%) were incorporated into the HA matrix. Among them, DHA 25% exhibited the highest antibacterial efficacy, with inhibition zones of 3.14 ± 0.51 cm² for *E. coli* and 7.07 ± 0.41 cm² for *S. aureus*, as shown in Tables 3.6 and 3.7.

The superior antibacterial activity of DHA 25% is attributed to the higher concentration of bioactive phytochemicals such as ellagic acid, gallic acid, and quercetin introduced through ethanol-based extraction. Phenolic compounds such as gallic acid and quercetin exert antibacterial effects through multiple mechanisms primarily targeting bacterial cell structures and functions. These compounds increase their lipophilicity, enabling them to interact strongly with bacterial cytoplasmic membranes, causing membrane destabilization and increased permeability, which leads to leakage of essential intracellular components. They also inhibit key bacterial enzymes and virulence factors, interfere with nucleic acid synthesis, and suppress biofilm formation. In Gram-positive bacteria like Staphylococcus aureus, phenolics can alter intracellular pH and disrupt energy generation by inhibiting ATP production, thereby impairing bacterial viability. Additionally, flavonoids can form complexes with proteins on bacterial cell walls and soluble proteins outside the cells, further inhibiting bacterial growth. Such multifaceted actions contribute to the potent bactericidal activity of phenolicrich plant extracts against pathogens including S. aureus and Escherichia coli. [36]. Ethanol efficiently extracts these active molecules, leading to better doping into the HA matrix [14]. Higher extract content also promotes sustained release of active agents due to improved diffusion kinetics, contributing to stronger inhibition zones. In contrast, lower concentrations may lack sufficient active compounds for prolonged antibacterial effects [6]. Additionally, Staphylococcus aureus (Grampositive) was more susceptible than Escherichia coli (Gramnegative), likely due to its porous peptidoglycan layer, which permits easier compound penetration, whereas the outer membrane of E. coli resists such penetration [37]. The antibacterial activity of DHA 25% showed inhibition zones of 7.07 ± 0.41 cm² (approximately 30 mm diameter) against Staphylococcus aureus and 3.14 ± 0.51 cm² (approximately 20 mm diameter) against Escherichia coli. In comparison, standard antibiotics such as ciprofloxacin typically produce inhibition zones around 22-28 mm for S. aureus and 29-35 mm for E. coli, while gentamicin zones are approximately 12-16 mm for S. aureus and 20-21 mm for E. coli [42]. This indicates that DHA 25% exhibits antibacterial efficacy comparable to or

Table 4. Antibacterial activity of different concentration of

Sample	Concentration of crude extract of <i>E. tirucalli</i>	Diameter of inhibition zone (cm)	Inhibition Zone (cm ²)	Solvent	Concentration of crude extract of <i>E. tirucalli</i>	Diameter of inhibition zone (cm)	Inhibition zone (cm²)
DHA 5%	5 mg/mL	1.3	1.33 ± 0.3	DHA 5%	5 mg/mL	2.8	6.15 ± 0.03
DHA 15%	15 mg/mL	1.4	1.54 ± 0.12	DHA 15%	15 mg/mL	2.9	6.61 ± 0.21
DHA 25%	25 mg/mL	2.0	3.14 ± 0.51	DHA 25%	25 mg/mL	3.0	7.07 ± 0.41
Antibiotic	5 mg/mL	5.0	19.625 ± 0.01	Antibiotic	5 mg/mL	4.0	6.28 ± 0.22
Pure HA	0 mg/mL	0.0	Null	Negative control HA	0 mg/mL	0.0	Null

exceeding that of some clinical antibiotics against *S. aureus* and is competitive against *E. coli*. These results highlight the potential of DHA 25% as an effective antimicrobial agent in biomedical applications, providing natural, sustained antibacterial activity with promising performance relative to established antibiotics. Overall, DHA 25% demonstrates potent, broad-spectrum antibacterial potential suitable for biomedical applications

3.6 Cytotoxicity

The cytotoxicity and biocompatibility of doped hydroxyapatite (DHA) were evaluated using the MTT assay, a standard method that measures cell metabolic activity and viability [38]. Figure 3.5 and Table 3.6 summarize the viability of cells cultured with pure HA and DHA containing 5%, 15%, and 25% concentrations of *Euphorbia tirucalli* extract over seven days.

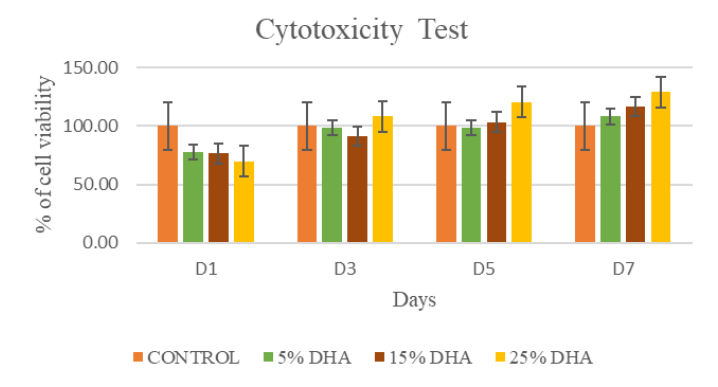


Fig. 5. Histogram of cell viability with the MTT method on HA and DHA

At the early time points (D0 and D1), all groups exhibited similarly low viability values (\leq 7.0 \pm 0.5), as shown in Table 3.6, confirming that both pure HA and DHA were initially nontoxic to cells. This uniform baseline (Figure 3.5) indicates that incorporation of *E. tirucalli* extract did not induce any acute cytotoxic stress. By day 3, viability increased modestly across all samples (\approx 11–14%), with no statistically significant differences among groups, suggesting consistent short-term biocompatibility regardless of doping concentration.

Table 6. Cell Viability of Pure Hydroxyapatite (HA) and Doped Hydroxyapatite (DHA) Over Time

Time (Days)	HA (Mean	5% (Mean	15% (Mean ±	25% (Mean ±
	± SD)	± SD)	SD)	SD)
$\mathbf{D0}$	0.0 \pm	0.0 \pm	$0.0\pm0.0^{\mathrm{a}}$	$0.0\pm0.0^{\mathrm{a}}$
	0.0^{a}	0.0^{a}		
D1	7.0 ±	5.0 ±	$6.0\pm0.5^{\rm a}$	$5.0\pm0.7^{\rm a}$
	0.5^{a}	0.6^{a}		
D3	12.0 ±	11.0 ±	12.0 ±	14.0 ±
	0.8^{a}	1.0^{a}	0.9^{a}	1.1a
D5	36.0 ±	37.0 ±	37.0 ±	43.0 ±
	2.0^{a}	1.8a	2.1a	2.4 ^b
D7	93.0 ±	106.0 ±	109.0 ±	120.0 ±
	4.2a	4.6 ^b	4.8 ^b	5.3°

Data are presented as mean \pm standard deviation (n = 3). Mean values in the same row with different superscript letters indicate significant differences at p < 0.05.

From day 5 onward, a marked increase in cell viability was observed in the DHA 25% group, suggesting that higher concentrations of *E. tirucalli* extract promote cell proliferation and alleviate cytotoxic stress over time. By day 7, DHA 25% reached the highest viability (120.0 \pm 5.3), significantly exceeding pure HA (93.0 \pm 4.2) as well as the 5% and 15% groups. These findings are consistent with [40], who reported that E. tirucalli enhances cell viability through modulation of antioxidant gene expression, and with [41], who demonstrated concentration-dependent improvements in cellular responses to E. tirucalli extracts. The enhanced cytocompatibility at 25% may be attributed to phytochemicals such as gallic acid, ellagic acid, and quercetin, known for their antioxidant and cytoprotective roles. Collectively, these results highlight DHA 25% as a promising candidate for biomedical applications where improved cytocompatibility is essential.

investigating high concentrations phytochemicals report dose-dependent cytotoxic effects on healthy cells, often linked to apoptosis induction and oxidative stress modulation. For instance, an ethyl acetate extract of Quercus infectoria rich in tannins, flavonoids, and phenolic compounds exhibited potent cytotoxicity against cancerous cell lines (IC50 \approx 6.33 µg/mL) but showed selective toxicity, sparing normal fibroblast (L929) cells at comparable concentrations [43]. This suggests that while phytochemicals have anticancer properties, their toxicity risk to healthy cells depends on concentration and exposure duration, with cytoselective effects possible. Other reviews emphasize that phytochemical toxicity arises primarily from oxidative damage, interaction with cellular macromolecules, or apoptosis pathways, necessitating careful dose evaluation, particularly for clinical or biomedical applications involving healthy tissue exposure. Therefore, although Euphorbia tirucalli extract doping enhances antibacterial and regenerative properties, future toxicological risk assessments should utilize systematic dose-response cytotoxicity testing on relevant healthy cell types to ensure safety at high phytochemical concentrations used in the biomaterial.

In terms of variance, the relatively small standard deviations across all groups indicate that the trends in viability were consistent and reproducible across replicates. Although slight variability was observed (e.g., D7 values ranging from ± 4.2 to ± 5.3), the overlap was minimal, and statistical analysis confirmed significant differences at higher concentrations. This suggests that the observed increase in cell viability, particularly in DHA 25%, reflects a true biological effect rather than random variation.

Overall, the MTT assay data provide preliminary evidence that incorporation of *E. tirucalli* extract, especially at 25%, enhances short-term cytocompatibility of HA. However, it must be emphasized that MTT alone cannot fully predict long-term biocompatibility or immune response. Further in-depth toxicological and immunological assessments, including dose response studies on relevant healthy cell lines and in vivo models, are required to confirm the safety and suitability of DHA for biomedical applications.

4. CONCLUSION

This study explored the extraction and biomedical application of Euphorbia tirucalli L. extract incorporated into hydroxyapatite (HA). Aqueous ethanol was the most effective solvent, yielding a Total Phenolic Content (TPC) of 2.501 \pm 0.50 mg GAE/g and a Total Flavonoid Content (TFC) of 1.307 ± 0.11 mg QE/g. HPLC analysis identified gallic acid as the dominant phenolic compound (557.9 ± 8.3 mg/g). Incorporating the extract into HA, particularly at 25%, enhanced antibacterial activity, showing inhibition zones of 7.07 ± 0.41 cm² against Staphylococcus aureus and 3.14 ± 0.51 cm² against Escherichia coli, values comparable to or exceeding those of many metal-ion doped commercial HA products. The MTT assay confirmed biocompatibility with a $120.0 \pm 5.3\%$ viability rate on day 7, indicating superior cytocompatibility over some conventional doped HA materials known for potential cytotoxic effects. Structural analyses via XRD and FTIR confirmed successful doping, while FESEM revealed reduced porosity and increased agglomeration correlating with modified surface area and pore size beneficial for osteointegration. These results support DHA 25% as a promising candidate for bone regeneration applications with multifunctional antibacterial and osteoinductive properties.

The real-world implications of this study highlight DHA 25%'s potential to reduce implant-associated infections and promote bone healing through natural bioactive compounds, addressing safety concerns linked to metal ion doping. Clinically, this material could improve patient outcomes by balancing antimicrobial efficacy with biocompatibility. Future research should focus on in vivo testing to validate long-term biocompatibility and bone regenerative capacity, as well as mechanical property evaluations to ensure suitability for load-bearing applications. This comprehensive approach paves the way for the integration of plant-based bioactive dopants into HA, offering a sustainable, multifunctional solution for next-generation bone biomaterials.

5. DECLARATION OF COMPETING INTEREST

This is to certify that we do not have any competing financial interests or personal relationships that could have appeared to influence the work reported in this paper. The authors do not have any conflict of interest also.

6. ACKNOWLEDGMENTS

The authors would like to thank the Ministry of Higher Education Malaysia for the support from the Fundamental Researchs Grant Scheme (FRGS) FRGS/1/2021/TK0/UNIMAP/02/59.

REFERENCES

- [1] Abbasi, M., Rashnavadi, M., Gholami, M., & Molaei, S. (2025). Antibacterial property of hydroxyapatite extracted from biological sources and doped with Cu2+ and Ag+ by Sol-gels method. Scientific Reports, 15(1). doi: https://doi.org/10.1038/s41598-025-89886-1
- [2] Mondal, S., Park, S., Choi, J., Vu, T. T. H., Doan, V. H. M., Vo, T. T., Lee, B., & Oh, J. (2023). Hydroxyapatite: A journey from biomaterials to advanced functional materials. Advances in Colloid and Interface Science, 321, 103013. doi: https://doi.org/10.1016/j.cis.2023.103013
- [3] Kauke-Navarro, M., Knoedler, L., Knoedler, S., & Safi, A. F. (2024). Advancements in facial implantology: a review of hydroxyapatite

- applications and outcomes. Frontiers in Surgery, 11. doi: https://doi.org/10.3389/fsurg.2024.1409733
- [4] Wang, X., Huang, S., & Peng, Q. (2023). Metal Ion-Doped Hydroxyapatite-Based materials for bone defect restoration. Bioengineering, 10(12), 1367. doi: https://doi.org/10.3390/bioengineering10121367
- [5] Araújo, K., De Lima, A., Silva, J., Rodrigues, L., Amorim, A., Quelemes, P., Santos, R. D., Rocha, J., De Andrades, É., Leite, J., Mancini-Filho, J., & Da Trindade, R. (2014). Identification of phenolic compounds and evaluation of antioxidant and Antibacterial properties of euphorbia TirucalliE.tirucalli L. Antioxidants, 3(1), 159–175. doi: https://doi.org/10.3390/antiox3010159
- [6] Oliveira, F. L., Lisboa-Filho, P. N., Ferreira, S. A., Tronto, J., Rossi, A. M., Oliveira, A. M., & Lima, E. C. (2020). Synthesis of hydroxyapatite nanoparticles via wet chemical precipitation: Influence of phosphate concentration and aging time. Materials Chemistry and Physics, 244, 122718. doi: https://doi.org/10.1016/j.matchemphys.2020.122718
- [7] Palit, P., Mukherjee, D., Mahanta, P., Shadab, M., Ali, N., Roychoudhury, S., Asad, M., & Mandal, S. C. (2020). Attenuation of nociceptive pain and inflammatory disorders by total steroid and terpenoid fraction of Euphorbia tirucalli Linn root in experimental in vitro and in vivo model. Inflammopharmacology, 26(1), 235–250. doi: https://doi.org/10.1007/s10787-017-0403-7
- [8] Mohammad, N. F., Yeoh, F. Y., & Othman, R. (2023). Synthesis of nanoporous carbonated hydroxyapatite using Non-Ionic pluronics surfactant. Advanced Materials Research, 686, 33–43. doi: https://doi.org/10.4028/www.scientific.net/amr.686.33
- [9] Le, N. T. M., Cuong, D. X., Van Thinh, P., Minh, T. N., Manh, T. D., Duong, T. H., Minh, T. T. L., & Oanh, V. T. T. (2021). Phytochemical screening and evaluation of antioxidant properties and Antibacterial activity against Xanthomonas axonopodis of Euphorbia tirucallie.tirucalli extracts in Binh Thuan Province, Vietnam. Molecules, 26(4), 941. doi: https://doi.org/10.3390/molecules26040941
- [10] Paolini, A. et al. (2020) MicroRNAs delivery into human cells grown on 3D-printed PLA scaffoldscoated with a novel fluorescent PAMAM dendrimer for biomedical applications, Scientific Reports,8(1), pp. 1–12. doi: https://doi.org/10.1038/s41598-018-32258-9
- [11] Gregor, A. et al. (2021) Designing of PLA scaffolds for bone tissue replacement fabricated byordinary commercial 3D printer, Journal of Biological Engineering, 11(1), pp. 1–21. doi: https://doi.org/10.1186/s13036-017-0074-3
- [12] Kilic, I., Yeşiloğlu, Y., & Bayrak, Y. (2024). Spectroscopic studies on the antioxidant activity of ellagic acid. Spectrochimica Acta Part A: Molecular and Biomolecular Spectroscopy, 130, 447–452. doi: https://doi.org/10.1016/j.saa.2014.04.052
- [13] Jin, N., Zhang, S., Sun, S., Wu, M., Yang, X., Xu, J., Ma, K., Guan, S., & Xu, W. (2022). An Organic Solvent-Free Method for the Extraction of Ellagic Acid Compounds from Raspberry Wine Pomace with Assistance of Sodium Bicarbonate. Molecules, doi: https://doi.org/10.3390/molecules27072145
- [14] Singh, M., Jha, A., Kumar, A., Hettiarachchy, N., Rai, A. K., & Sharma, D. (2024). Influence of the solvents on the extraction of major phenolic compounds (punicalagin, ellagic acid and gallic acid) and their antioxidant activities in pomegranate aril. Journal of Food Science and Technology, 51(9), 2070–2077. doi: https://doi.org/10.1007/s13197-014-1267-0
- [15] Xu, D., Hu, M., Wang, Y., & Cui, Y. (2021). Antioxidant activities of quercetin and its complexes for medicinal application. Molecules, 24(6),1123. doi: https://doi.org/10.3390/molecules24061123
- [16] Pham-Huy, L. A., He, H., & Pham-Huy, C. (2023). Free radicals, antioxidants in disease and health. International Journal of Biomedical Science, 4(2), 89–96. doi: https://doi.org/10.59566/ijbs.2008.4089
- [17] Baskaran, T., Mohammad, N. F., Saleh, S. S. M., Nasir, N. F. M., & Daud, F. D. M. (2021). Synthesis Methods of Doped Hydroxyapatite: A Brief Review. Journal of Physics: Conference Series, 2071(1). doi: https://doi.org/10.1088/1742-6596/2071/1/012008
- [18] Martinez-Zelaya, V. R. Z. L., Herrera, E. Z., Alves, A. T., Uzeda, M. J., Mavropoulos, E., Rossi, A. L., Mello, A., Granjeiro, J. M., Calasans-Maia, M. D., & Rossi, A. M. (2020). In vitro and in vivo evaluations of nanocrystalline Zn-doped carbonated hydroxyapatite/alginate microspheres: Zinc and calcium bioavailability and bone regeneration.

- International Journal of Nanomedicine, 14, 3471-90. doi: https://doi.org/10.2147/IJN.S197157
- [19] Sprio, S., Dapporto, M., Preti, L., Mazzoni, E., Iaquinta, M.R., Martini, F., Tognon, M., Pugno, N.M., Restivo, E., Visai, L. and Tampieri, A., (2020). Enhancement of the biological and mechanical performances of sintered hydroxyapatite by multiple ions doping. Frontiers in Materials, 7, p.224. doi: https://doi.org/10.3389/fmats.2020.00224
- [20] Dorozhkin, S. V. (2020). Calcium orthophosphates as bioceramics: State of the art. Journal of Functional Biomaterials, 1(1), 22–107. doi: https://doi.org/10.3390/jfb1010022
- [21] Vallet-Regí, M., & González-Calbet, J. M. (2024). Calcium phosphates as substitution of bone tissues. Progress in Solid State Chemistry, 32(1– 2), 1–31. doi: https://doi.org/10.1016/j.progsolidstchem.2004.07.001
- [22] Kumar, N., & Goel, N. (2022). Phenolic acids: Natural versatile molecules with promising therapeutic applications. Biotechnology Reports, 24, e00370. doi: https://doi.org/10.1016/j.btre.2019.e00370
- [23] Venkatesan, J., & Kim, S. K. (2020). Chitosan s for bone tissue engineering—An overview. Marine Drugs, 8(8), 2252-2266
- [24] Sadat-Shojai, M., Khorasani, M.-T., Dinpanah-Khoshdargi, E., & Jamshidi, A. (2023). Synthesis methods for hydroxyapatite nanoparticles. Acta Biomaterialia, 9(8), 7591-7621. doi: https://doi.org/10.1016/j.actbio.2013.04.01
- [25] Heya, M. S., Verde-Star, M. J., Rivas-Morales, C., García-Hernández, D. G., Tijerina-Sáenz, A., López-Cabanillas-Lomelí, M., Álvarez-Román, R., & Galindo-Rodríguez, S. A. (2024). In vitro antifungal activity of polymeric nanoparticles loaded with Euphorbia tirucallie.tirucalli extract. Brazilian Journal of Biology, 84. doi: https://doi.org/10.1590/1519-6984.275974
- [26] Khang, N. V. D., Nhi, N. T. Y., & Quan, T. L. (2023). Potential biofuel exploitation from two common Vietnamese Euphorbia plants (Euphorbiaceae). Biofuels, Bioproducts and Biorefining, 17(5), 1315– 1327. doi: https://doi.org/10.1002/bbb.2472
- [27] Karageorgiou, V., & Kaplan, D. (2025). Porosity of 3D biomaterial scaffolds and osteogenesis. Biomaterials, 26(27), 5474–5491. doi: https://doi.org/10.1016/j.biomaterials.2005.02.002
- [28] Collins, M. N., Ren, G., Young, K., Pina, S., Reis, R. L., & Oliveira, J. M. (2021). Scaffold fabrication technologies and Structure/Function properties in bone tissue engineering. Advanced Functional Materials, 31(21). doi: https://doi.org/10.1002/adfm.202010609
- [29] Thommes, M., Kaneko, K., Neimark, A. V., Olivier, J. P., Rodriguez-Reinoso, F., Rouquerol, J., & Sing, K. S. (2025). Physisorption of gases, with special reference to the evaluation of surface area and pore size distribution (IUPAC Technical Report). Pure and Applied Chemistry, 87(9–10), 1051–1069. doi: https://doi.org/10.1515/pac-2014-1117
- [30] Bose, S., Roy, M., & Bandyopadhyay, A. (2022). Recent advances in bone tissue engineering scaffolds. Trends in Biotechnology, 30(10), 546-554. doi: https://doi.org/10.1016/j.tibtech.2012.07.005
- [31] Calzaferri, G., Gallagher, S. H., Lustenberger, S., Walther, F., & Brühwiler, D. (2022). Multiple equilibria description of type H1 hysteresis in gas sorption isotherms of mesoporous materials. Materials Chemistry and Physics, 296, 127121. doi: https://doi.org/10.1016/j.matchemphys.2022.127121
- [32] Yadav, P., Beniwal, G., & Saxena, K. K. (2021). A review on pore and porosity in tissue engineering. Materials Today Proceedings, 44, 2623– 2628. doi: https://doi.org/10.1016/j.matpr.2020.12.661
- [33] Nirmala, R. & Sheikh, Faheem & Kanjwal, Muzafar & Lee, John & Park, Soo-Jin & Navamathavan, R. & Kim, Hak. (2021). Synthesis and characterization of bovine femur bone hydroxyapatite containing silver nanoparticles for the biomedical applications. Journal of Nanoparticle Research. 13. 1917-1927. doi: https://doi.org/10.1007/s11051-010-9944-z
- [34] Wang, L., & Nancollas, G. H. (2022). ChemInForm Abstract: Calcium Orthophosphates: Crystallization and Dissolution. ChemInform, 40(5). doi: https://doi.org/10.1002/chin.200905233
- [35] Gayathri, B., Muthukumarasamy, N., Velauthapillai, D., Santhosh, S., & Asokan, V. (2020). Magnesium incorporated hydroxyapatite nanoparticles: Preparation, characterization, antibacterial and larvicidal activity. Arabian Journal of Chemistry, 11(5), 645–654. doi: https://doi.org/10.1016/j.arabjc.2016.05.010

- [36] Prasad, Swapna, N., & Prasad, M. (2021). Efficacy of Euphorbia tirucalliE.tirucalli (L.) towards microbicidal activity against human pathogens. International Journal of Pharma and Bio Sciences. doi: http://www.ijpbs.net/volume2/issue1/biological/_32.pdf
- [37] Tahara, Y. O., & Miyata, M. (2023). Visualization of Peptidoglycan Structures of E.coli by Quick-Freeze Deep-Etch Electron Microscopy. METhods in Molecular Biology, 299–307. doi: https://doi.org/10.1007/978-1-0716-3060-0_24
- [38] Sobierajska, P., Serwotka-Suszczak, A., Targonska, S., Szymanski, D., Marycz, K., & Wiglusz, R. J. (2022). Synergistic Effect of toceranib and Nanohydroxyapatite as a Drug Delivery Platform—Physicochemical properties and in vitro studies on mastocytoma cells. International Journal of Molecular Sciences, 23(4), 1944. doi: https://doi.org/10.3390/ijms23041944
- [39] Khan, B., Jabeen, K., Kanwal, Q., & Iqbal, S. (2021). Phytochemical constituents of pencil tree (Euphorbia tirucalli) as an antifungal agent against mango anthracnose disease. Applied Ecology and Environmental Research, 19(4), 2915–2928. doi: https://doi.org/10.15666/aeer/1904_29152928
- [40] Waczuk, E. P., Kamdem, J. P., Abolaji, A. O., Meinerz, D. F., Bueno, D. C., Gonzaga, T. K. S. D. N., Dorow, T. S. D. C., Boligon, A. A., Athayde, M. L., Da Rocha, J. B. T., & Ávila, D. S. (2025). Euphorbia tirucalliE.tirucalli aqueous extract induces cytotoxicity, genotoxicity and changes in antioxidant gene expression in human leukocytes. Toxicology Research, 4(3), 739–748. doi: https://doi.org/10.1039/c4tx00122b
- [41] Silva, V., Rosa, M., Tansini, A., Oliveira, R., Martinho, O., Lima, J. P., Pianowski, L., & Reis, R. (2022). In vitro screening of cytotoxic activity of euphol from Euphorbia tirucalliE.tirucalli on a large panel of human cancer derived cell lines. Experimental and Therapeutic Medicine. doi: https://doi.org/10.3892/etm.2018.6244
- [42] Mukhtar, M. D., Rufa'i, F. A., Yola, A. U., Babba, N. I., & Baecker, D. (2023). Evaluating the potency of selected antibiotic medications dispensed in community pharmacies in Gwale, Kano, Nigeria. Antibiotics, 12(11), 1582. doi: https://doi.org/10.3390/antibiotics12111582
- [43] Yusof, W. N. S. W., & Abdullah, H. (2020). Phytochemicals and Cytotoxicity of Quercus infectoria Ethyl Acetate Extracts on Human Cancer Cells. Tropical Life Sciences Research, 31(1), 69–84. doi: https://doi.org/10.21315/tlsr2020.31.1.5
- [44] Akhter, M. S., Rahman, M. A., Ripon, R. K., Mubarak, M., Akter, M., Mahbub, S., Mamun, F. A., & Sikder, M. T. (2024). A systematic Review on Green Synthesis of Silver Nanoparticles Using Plants Extract and Their Bio-medical Applications. Heliyon,10(11),29766. doi: https://doi.org/10.1016/j.heliyon.2024.e29766
- [45] Wylie, M. R., & Merrell, D. S. (2022). The Antimicrobial Potential of the Neem Tree Azadirachta indica. Frontiers in Pharmacology, 13. doi: https://doi.org/10.3389/fphar.2022.891535